JOURNAL OF MATERIALS SCIENCE 23 (1988) 1709–1717

Structural and electrical properties of the glassy semiconductor system Cu–As–Te

Part 2 *Structural analysis by X-ray diffraction and space models*

J. VÁZQUEZ, E. MÁRQUEZ, N. DE LA ROSA-FOX, P. VILLARES, R. JIMÉNEZ-GARAY
Departamento de Física Fundamental, Facultad de Ciencias, Universidad de Cádiz, Apartado 40, Puerto Real (Cádiz), Spain

An X-ray diffraction radial-distribution study of $Cu_{0.05}As_{0.50}Te_{0.45}$ (MI) and $Cu_{0.15}As_{0.40}Te_{0.45}$ (MII) amorphous alloys obtained by the melt-quench method has been performed. The short-range order proposed from the radial distribution function (RDF) interpretation was calculated from a theoretical expression that takes into account the variation with s (scattering vector modulus) of the atomic scattering factor, and approximating it to polynomial functions. The local order of both alloys presents a deviation from the covalent character of the arsenic and tellurium elements bound to copper, increasing the mean coordination and not fitting the "octet" rule. For an in-depth study of the structural characteristics, tridimensional models were built by computer simulation of an X-ray diffraction experiment. Refinement was carried out by the Metropolis–Monte Carlo method with some modifications. The basic structure of both models may be described by a network of tetrahedra centred on copper and arsenic atoms. As both clusters are intermingled, the network connectivity is increased. Both models present a certain number of tellurium atoms with dangling bonds with average bonding distances above the mean value in the model which, together with the copper concentration, may be responsible for its decreased electrical resistivity.

1. Introduction

Chalcogenide glasses are in general characterized by high values of resistivity, implying certain limitations in their applications as well as difficulty in electrical measurements. Borisova [1] has shown that the addition of some d-elements in amorphous materials can lead to significant changes in their resistivities. On the other hand, these materials are studied mainly because they present switching phenomena and memory effects and therefore can be used in the manufacture of a great number of electronic devices [2].

Of these glasses, those containing tellurium are characterized by their high electrical conductivity, this property being heightened when one of the elements of the material is copper. The relationship between electrical conductivity and sample composition in this type of ternary alloy is one of the reasons justifying the interest in establishing both the structural and electrical properties of the Cu–As–Te system.

A structural analysis, with a view to a later study of their electrical properties, has been carried out in the $Cu_{0.05}As_{0.50}Te_{0.45}$ (MI) and $Cu_{0.15}As_{0.40}Te_{0.45}$ (MII) alloys of the aforementioned system, given that the establishment of structural units, the distribution of chemical bonds between atoms, the radii of coordination spheres and the mean values of the bond distances, besides having an intrinsic interest, can provide an explanation of how the process of electrical conductivity in this system is so closely related to the type and amount of chemical bonds present in the material.

In the present paper, the results of the atomic radial distribution study are extended by means of the simulation of tridimensional models, which permit a statistical analysis of the main structural parameters, as well as justifying some of its macroscopic properties.

2. Experimental procedure

Samples of the MI and MII alloys were prepared with commercial copper, arsenic and tellurium elements of 5 N nominal purity, appropriate proportions of which were mixed homogeneously to obtain the aforementioned compositions. The mixtures were placed in quartz ampoules which were hermetically sealed in an inert helium atmosphere. The sample-containing ampoules were placed in a rotatory furnace at 900° C for 4 h, after which the ampoules were rapidly air-cooled.

In both cases, part of the prepared solid was powdered to particle size less than 325 mesh, and compressed into pastille shapes of 30 mm × 12 mm × 1 mm. The absence of peaks typical of a crystalline phase was verified by X-ray diffraction.

The density of each alloy was determined experimentally by a pycnometric method at constant temperature. The mean values obtained for MI and MII were 5.44 and 5.80 $g\,cm^{-3}$, respectively.

0022–2461/88 $03.00 + .12

Diffracted radiation intensities were determined with an automatic powder diffractometer (Siemens D500) that verifies the Bragg–Brentano geometry by reflection. Mo K_α radiation ($\lambda = 0.071069$ nm) was selected by means of a bent graphite monochromator, and radiation was detected with a scintillation counter fitted with a photosensitive NaI(Tl) window.

To obtain scattering intensities, four series of measurements were taken in the interval $5° \leqslant 2\theta \leqslant 110°$, two each for increasing and decreasing scattering angles. These measurements were based on the determination of the time taken in registering a set number of counts ($n = 4000$).

3. Theory

From the structural information that is obtained from experimental intensities, the radial atomic distribution is deduced, from which the short-range order of the material may be postulated.

Reduced intensity, as a function of the scattering vector modulus $s = (4\pi/\lambda) \sin \theta$, is defined as

$$i(s) = \frac{I_{\text{e.u.}}(s) - \sum_i x_i f_i^2(s)}{\left[\sum_i x_i f_i(s)\right]^2} \quad (1)$$

where $I_{\text{e.u.}}(s)$ is the coherent part of the measured intensity, corrected and normalized to electron units (e.u.), and x_i and $f_i(s)$ are, respectively, the atomic fraction and the atomic scattering factor of an i-type atom.

The pair correlation function (PCF) is obtained from the Fourier transform of the interference function, $F(s) = si(s)$, as

$$G(r) = \frac{2}{\pi} \int_0^{s_m} F(s) \sin (sr)\, ds \quad (2)$$

where s_m is the upper measurement limit, which generates the radial distribution function (RDF) given by

$$4\pi r^2 \varrho(r) = 4\pi r^2 \varrho_0 + rG(r) \quad (3)$$

where $\varrho(r)$ is local atomic density, affected by the Fourier transform of the products $R_{ij}(s) = f_i(s)f_j(s)/[\Sigma_i x_i f_i(s)]^2$, and ϱ_0 is the average experimental atomic density of the material, expressed in atoms per unit volume.

The RDF, as a probability function, provides information on the average number of atomic centres around an arbitrary one taken as reference. Thus, this function presents maxima in the positions of these centres. The area below each peak provides the average number of neighbours of each coordination sphere.

One of these areas, that corresponding to the first peak, is related to certain structural parameters which may be used to propose an average structural model of the material. The following relation may be used in many cases:

$$\text{Area} = \frac{1}{\left(\sum_i x_i Z_i\right)^2} \sum_i \sum_j n_{ij} x_i Z_i Z_j \quad (4)$$

in which Z_i and Z_j are the atomic numbers of Elements i and j, respectively, and n_{ij} the structural parameters representing the average numbers of j-type atoms surrounding an arbitrary i-type atom in the first coordination sphere, i.e. the mean relative coordination number.

Nevertheless, the previous relation is only valid when the $R_{ij}(s)$ functions remain practically constant and equal to $Z_i Z_j/(\Sigma_i x_i Z_i)^2$, in the complete s interval in which the measurements are carried out. When the $R_{ij}(s)$ functions move significantly away from these constant values, Vázquez and Sanz [3] have deduced a more approximate expression for the area of the first peak of the RDF, following the method described by Warren [4] and considering that the products $R_{ij}(s)$ may be approximated by n-order polynomials in s. This expression is

$$\text{Area} = \frac{2}{\pi} \sum_i \sum_j x_i \frac{n_{ij}}{r_{ij}} \int_b^a r P_{ij}(r)\, dr \quad (5)$$

where r_{ij} is the average distance between an i-type and a j-type atom, a and b are the limits of the first peak of the RDF and $P_{ij}(r)$ a function defined by

$$P_{ij}(r) = \frac{1}{2} \int_0^{s_m} \frac{f_i(s) f_j(s)}{\left[\sum_i x_i f_i(s)\right]^2} \cos [s(r - r_{ij})]\, ds \quad (6)$$

The structural information obtained from the analysis of the experimental RDF, together with certain known physical-chemical properties of the compound and its constituting elements, allow a hypotheses on the short-range order of the alloy to be proposed. For an in-depth study of the stereochemistry of these materials, tridimensional structural models are generated numerically, and their analysis provides information on the main structural parameters (distances, bonding angles, packing, etc.).

From different methods found in the literature [5, 6] for the generation of structures of amorphous solids, the aleatory Metropolis–Monte Carlo method [7] seems the most appropriate for describing the short-range order of a material, as it best simulates the structural characteristics of an alloy obtained by sudden quenching of the molten mixture.

This method for the construction of structural models (modified because the lack of long-range order does not imply maximum aleatoriness of the atomic network) may be described as a two-step process: (i) generation of the initial atomic configuration, and (ii) refinement of the same.

In the first step a particular volume is chosen, and a number of positions are created within it equal to the number of atoms that may also be in it, according to the experimental density and atomic mass of the composition unit. The generation of positions is carried out in a semi-aleatory fashion taking into account the stereochemical hypotheses that are deduced from the analysis of the experimental RDF.

A theoretical diffraction experiment is carried out on the model with the object of calculating its reduced RDF, $rG_{\text{mod}}(r)$. This is then compared to the experimental RDF, $rG_{\text{exp}}(r)$, damped by a function simulating

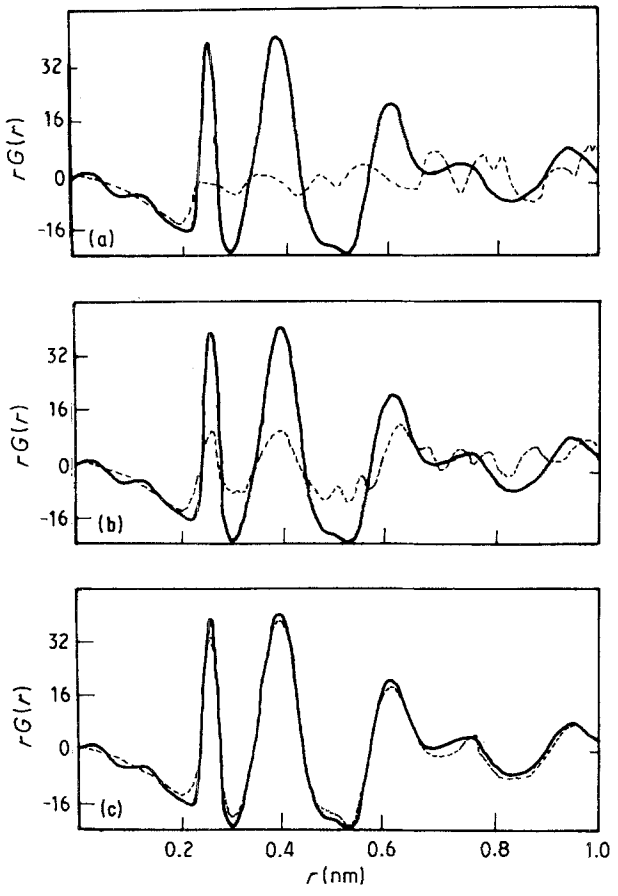

Figure 1 (– – –) $rG_{mod}(r)$ and (——) $rG(r)D(r)$ in some steps of the refinement process, for MI alloy.

the finite size of the model, which is defined as

$$D(r) = 1.0 - 1.5\left(\frac{r}{2R}\right) + 0.5\left(\frac{r}{2R}\right)^3 \quad (7)$$

proposed by Mason [8] that represents the probability of finding an r distance in a sphere of radius R. The mean quadratic deviation of both functions is given by the relation

$$\varepsilon^2 = \frac{1}{M}\sum_i [r_i G_{exp}(r_i) D(r_i) - r_i G_{mod}(r_i)]^2 \quad (8)$$

in which M is the number of points where the adjustment has been carried out. The value of this parameter is used as criterion of the model validity.

In the second step the positions of the model are refined, evolving through successive movements of the atoms in aleatory directions, but obeying the foreseen geometric and coordination restrictions. A movement is considered valid when the mean quadratic deviation is decreased.

Fine adjustment of positions is considered as being complete when the necessary computation time to effect a valid movement is excessive and the mean quadratic deviation between the reduced RDFs of the model and the experimental data does not undergo notable improvement. Values of ε^2 less than 0.05 give statistically significant models. In Fig. 1 the different stages of this process are shown, in which Fig. 1a corresponds to the initial configuration and shows the aleatoriness of the model, Fig. 1b to that after 100 valid movements when the definition of the first peaks is observed accounting for the very short-range order, and Fig. 1c to that when $\varepsilon^2 = 0.045$ and all the model's coordination spheres are defined and adjusted.

4. Results

4.1. RDF analysis and short-range order hypotheses

The intensities measured experimentally were corrected for background, polarization and multiple scattering, Warren's method [4] being used in the last correction. Compton scattering was evaluated, taking into account monochromator efficiency and following the procedure described by Shevchik [9]. The intensities were expressed in electron units by means of the high-angle method [4]. These intensities are shown in Fig. 2.

The $F(s)$ function was theoretically extended to $s_{max} = 300\,nm^{-1}$ to avoid spurious oscillations in $G(r)$ below the first significant maximum due to the lack of data for high s, with the method described by D'Anjou and Sanz [10] based on Shevchik's method [9], which supposes that for high s values the $F(s)$ function is approximated by

$$F_{theoretical}(s) = \frac{C}{r}\sin(rs)\,e^{-\sigma^2 s^2/2} \quad (9)$$

where C, r and σ are parameters obtained by the least-squares method from the initial C_1, r_1 and σ_1 values representing the area, position and half-width of the first peak of the RDF obtained from the Equation 2 for $s_m = 144.8\,nm^{-1}$, the maximum value in our experimental device.

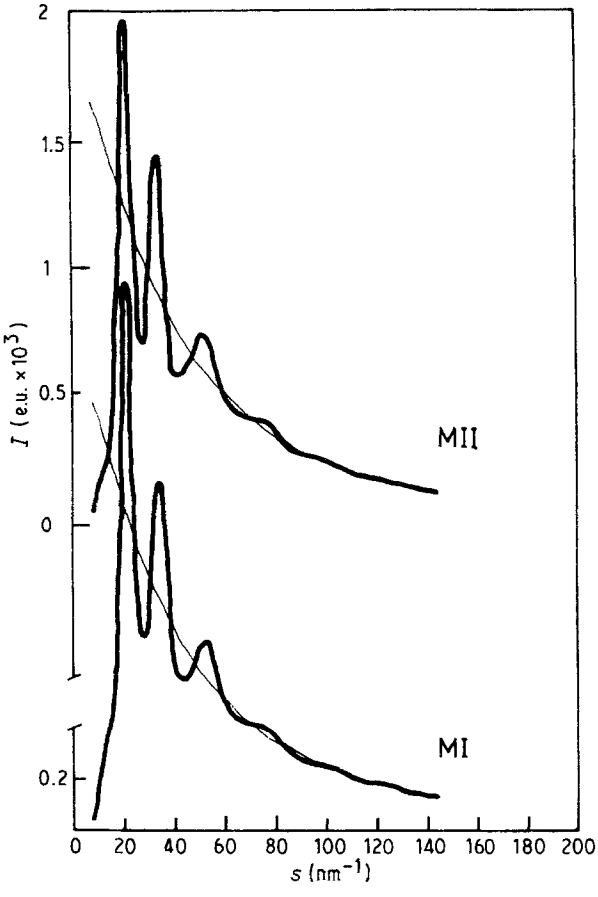

Figure 2 Normalized experimental intensities and structure-independent scattering curve (fine line) in electron units.

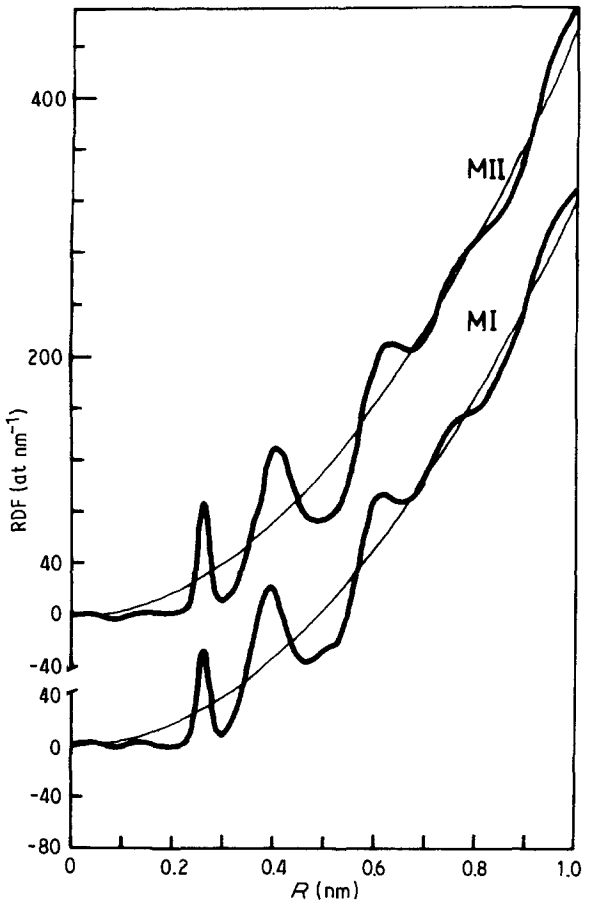

Figure 3 Radial distribution functions (RDFs).

The Fourier transform of the extended $F(s)$ functions gave rise to the RDFs of both alloys which have been plotted in Fig. 3. The analysis of the experimental RDFs of each compound gives the structural information summarized in Table I.

The definition interval of the first peak, corresponding to the first coordination sphere in each of the compositions of the Cu–As–Te system (Cu = 1, As = 2, Te = 3), is such that all types of bond between the different elements of both compounds are possible, as may be deduced from the comparison of the aforementioned intervals with the bonding lengths, found in the literature [11–15].

Taking into account that in these alloys tellurium contributes to a greater degree to the diffraction spectrum, it seems logical to think that the first maximum of the RDF is found between the values defining the bonding lengths of this element (Te–X), which agrees with the mean weighted value of these lengths (0.259 nm for MI, 0.260 nm for MII), in agreement with the positions of the first peak obtained experimentally (Table I).

As has been indicated previously, the area enclosed by the first peak of the RDF represents the mean coordination number of the material. Thus, it is of interest to theoretically evaluate this parameter. This may be done using the appropriate hypotheses, and comparing it to its experimental value when attempting to generate a structural model of the alloy.

In the case of the glassy system Cu–As–Te, copper is supposed to be tetracoordinated ($N = 4$), accepting the necessary electrons for sp^3 hybridization of some arsenic and tellurium atoms, which increase their coordination to become 4 and 3, respectively [11–16].

For the theoretical calculation of the area under the first peak of the RDF, bearing in mind previous hypotheses, the variation with s of the $R_{ij}(s)$ functions have been considered. To this end, the relation deduced by Vázquez *et al.* [17] has been used:

$$\text{Area} = \frac{1}{50\pi}[(h + \beta A_{22} - 2\delta A_{23})N + \alpha A_{22} + 2\gamma A_{23} + 2(A_{22} + A_{33} - 2A_{23})a_{33}] \quad (10)$$

where

$$h = \frac{a_1'}{100}[a_1' A_{11} + 2(a_2' A_{12} + a_3' A_{13}) + (a_3' - a_2')A_{22} - 2a_3' A_{23}] \quad (11)$$

and α, β, γ and δ are characteristic parameters of each alloy and a_{33} is the number of bonds between tellurium atoms and a_i' (i = d, 2, 3) is the concentration of i-element in 100 atoms of material.

For the determination of the A_{ij} parameters which figure in the previous expressions, the $R_{ij}(s)$ functions have been adjusted by the corresponding regression straight lines and, following the method described by Vázquez *et al.* [3] the values in Table II were calculated. The following results were obtained for the specific characteristics of each alloy: for MI

$$h = 3.2905 \quad \alpha = 64.63 \quad \beta = 0.37$$
$$\gamma = 85.68 \quad \delta = -2.32$$

and for MII

$$h = 10.5763 \quad \alpha = 35.53 \quad \beta = -0.53$$
$$\gamma = 80.24 \quad \delta = -7.76$$

With these parameters and the A_{ij} from Table II, by means of Equation 10 the area below the first peak of the RDF is given by

$$\text{Area} = 2.4090 + 0.0064\,a_{33} \quad (12)$$

TABLE I RDF characteristics

	Alloy MI		Alloy MII	
	Max. 1	Max. 2	Max. 1	Max. 2
Position (nm)	0.260	0.395	0.260	0.405
Limits (nm)	0.225 to 0.300	–	0.220 to 0.295	–
Averaged angle (deg.)	98.9		102.3	
Area (atoms)	2.44	6.97	2.86	7.05
Estimated error	±0.1	±0.2	±0.1	±0.2

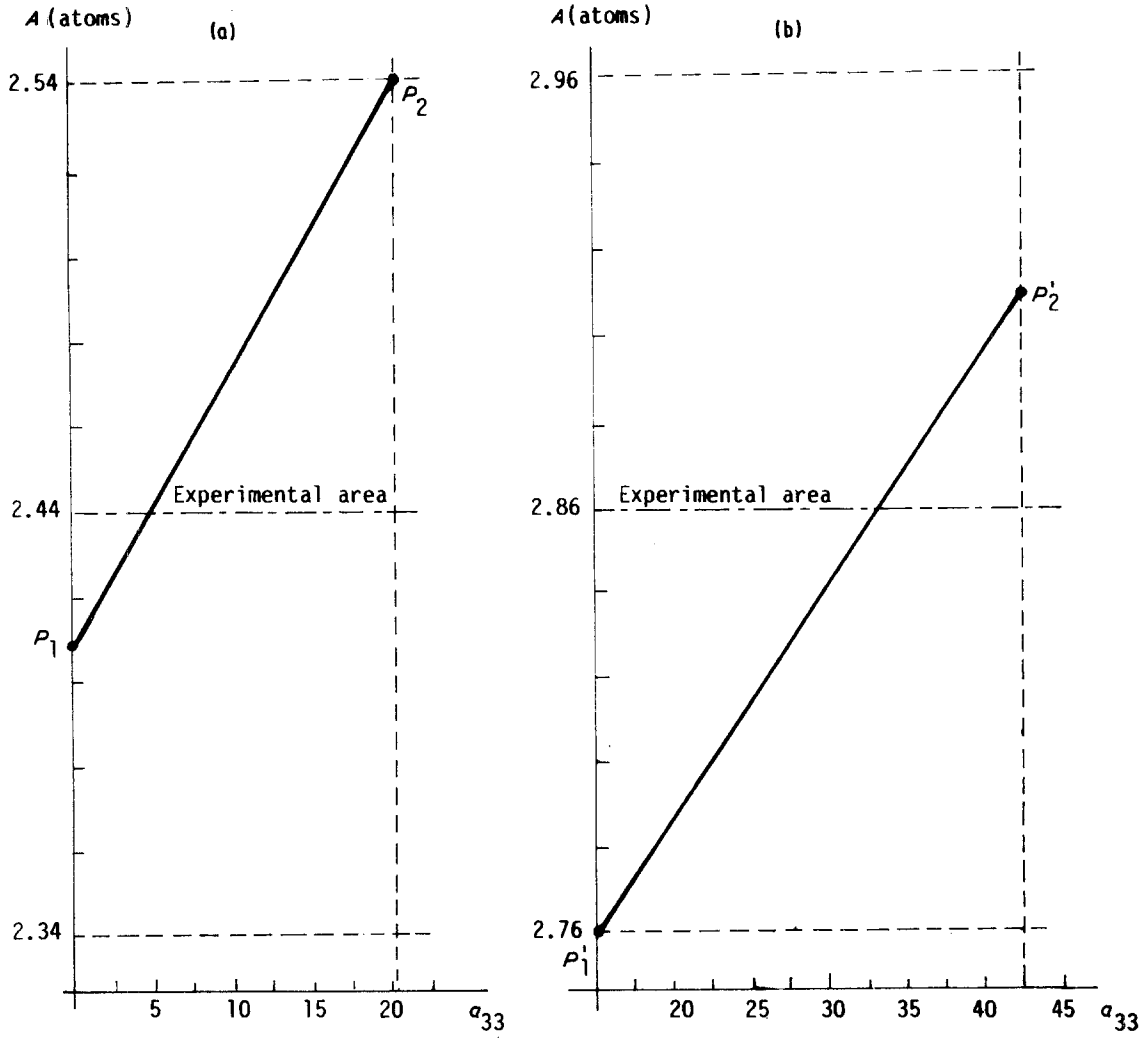

Figure 4 Area under first peak against number of Te–Te bonds for alloys (a) MI and (b) MII.

in the case of the first alloy (MI) and by

$$\text{Area} = 2.6766 + 0.0055\,a_{33} \qquad (13)$$

in the second (MII).

As can be seen, these functions vary linearly with the number of Te–Te bonds. These areas, against the variable a_{33} for each of the compositions, are shown in Fig. 4 and then compared to the experimental values, allowing the variable to be enclosed within the interval $0 \leqslant a_{33} \leqslant 20.47$ in the case of MI, and $15.16 \leqslant a_{33} \leqslant 42.45$ for MII.

Mean relative coordination numbers, n_{ij}, that depend on a_{33} [18], corresponding to the extremes of the intervals are shown in Table III.

Bearing in mind these n_{ij} values, it may be postulated that the material of each one of the samples possesses a short-range order between the indicated extreme situations, so that those models which verify the mean coordination numbers of the aforementioned extreme values may be postulated as the most probable structural models, and from which the mean number of bonds, a_{ij}, has been calculated for every 100 atoms of material (shown in Table IV).

In accordance with these suppositions and the n_{ij} established, structural models may be proposed for the glassy system Cu–As–Te in which, together with tetrahedral units centred on copper atoms, such as are shown below

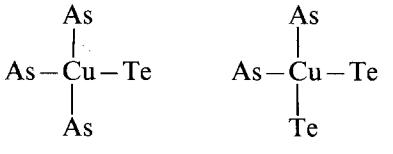

other tetrahedra centred on arsenic atoms coexist. All

TABLE II Functions $R_{ij}(s)$ and values obtained for A_{ij}

Pair	$R_{ij}(s)$		A_{ij}	
	MI	MII	MI	MII
1–1	$-7.6 \times 10^{-4} s + 0.4836$	$-7.6 \times 10^{-4} s + 0.4930$	0.7218	0.7329
1–2	$-7.3 \times 10^{-4} s + 0.5529$	$-7.3 \times 10^{-4} s + 0.5642$	0.8513	0.8443
1–3	$-3.7 \times 10^{-4} s + 0.8853$	$-3.5 \times 10^{-4} s + 0.9030$	1.3731	1.4113
2–2	$-6.8 \times 10^{-4} s + 0.6325$	$-6.8 \times 10^{-4} s + 0.6451$	1.0058	0.9614
2–3	$-1.3 \times 10^{-4} s + 1.0119$	$-1.1 \times 10^{-4} s + 1.0324$	1.5730	1.5545
3–3	$15.1 \times 10^{-4} s + 1.6166$	$15.9 \times 10^{-4} s + 1.6491$	2.6414	2.5777

TABLE III Coordination numbers corresponding to the extremes of the intervals for both alloys

	Coordination numbers		
Alloy MI			
$a_{33} = 0$	$n_{11} = 0.2$	$n_{12} = 2.04$	$n_{13} = 1.76$
	$n_{21} = 0.2$	$n_{22} = 1.27$	$n_{23} = 1.69$
	$n_{31} = 0.2$	$n_{32} = 1.96$	$n_{33} = 0$
$a_{33} = 20.47$	$n_{11} = 0.2$	$n_{12} = 2.04$	$n_{13} = 1.76$
	$n_{21} = 0.2$	$n_{22} = 2.07$	$n_{23} = 0.89$
	$n_{31} = 0.2$	$n_{32} = 1.03$	$n_{33} = 0.93$
Alloy MII			
$a_{33} = 15.16$	$n_{11} = 0.6$	$n_{12} = 1.64$	$n_{13} = 1.76$
	$n_{21} = 0.6$	$n_{22} = 1.60$	$n_{23} = 1.33$
	$n_{31} = 0.6$	$n_{32} = 1.24$	$n_{33} = 0.69$
$a_{33} = 42.45$	$n_{11} = 0.6$	$n_{12} = 1.64$	$n_{13} = 1.76$
	$n_{21} = 0.6$	$n_{22} = 2.93$	$n_{23} = 0$
	$n_{31} = 0.6$	$n_{32} = 0$	$n_{33} = 1.93$

these structural units would be linked by branched chains, constituted by an excess of arsenic and tellurium atoms.

4.2. Generation and analysis of structural models

In the two compositions studied of the Cu–As–Te system, the initial configuration of the atomic positions was generated in a space limited by a spherical surface of 1 nm radius in which were placed, in agreement with the density and composition of each alloy, 7 copper atoms, 72 arsenic atoms and 62 of tellurium in the case of MI, and 23 of copper, 62 of arsenic and 67 of tellurium for MII, imposing the geometrical restrictions that had been deduced from the respective experimental RDFs, referred to distances and bonding angles, and the condition in which the maximum number of first neighbours was no more than four.

The process of position adjustment was carried out by means of atomic shifts in aleatory directions. The values of amplitudes of these shifts were 0.03, 0.02 and 0.01 nm in the different stages of fitting. Movements implying the breakage of bonds of copper atoms were not allowed in this process, so that the coordination of this element could be maintained. The model corresponding to MI, after 580 valid movements, attained a mean quadratic deviation of 0.00171 nm, while for MII the deviation was 0.00215 nm after 629 valid movements. Thus, these models could be considered as representative of the structure of the materials under study, and the corresponding fitting process could be considered to be completed. Fig. 5 shows the reduced RDFs of the model and the experimental data for each of the alloys.

TABLE IV Mean number of bonds

Bond	a_{ij}	
	MI	MII
1–1	1	5
1–2	10	25
1–3	9	26
2–2	42	46
2–3	66	27
3–3	10	29

TABLE V Coordination in both models

Type of atom	Coordination				
	4	3	2	1	0
Cu	*7–23*	–	–	–	–
As	17–20	*23–29*	22–11	10–2	–
Te	–	12–14	*32–35*	15–15	3–2

Italics denote the number of atoms of each type having the usual coordination.

A comparative analysis of the principal structural parameters was carried out to extend our structural knowledge for the two alloys. The resultant coordination in both models is set out in Table V, where the first value corresponds to the model of the alloy MI and the second to the model of the alloy MII.

Arsenic and tellurium atoms present dangling bonds that, to a large extent, belong to atoms less than first-neighbour distance (78%) from the sphere periphery and could be satisfied with hypothetical external neighbours. In all, the number of over-coordinated atoms is similar to that of under-coordinated ones in both models. These defects are taken into consideration by the term "valence alternation pairs" (VAP) described by Kastner *et al.* [19], with a much smaller creation energy than the energy to break a bond, and has as a consequence a relative density of loaded defects present in the material in equilibrium, which produces a Fermi level pinned in the gap. Given the similarity of coordination distribution in both models, it may be concluded that the electrical behaviour of each alloy as an intrinsic semiconductor will also be similar. In any case, the

TABLE VI Averaged bonding distances

Bond	$\langle d_{ij} \rangle$ (nm)	Ref.
Cu–Cu	0.289	*
	0.251	†
	0.258	‡
Cu–As	0.260	*
	0.255	†
	0.253	§
Cu–Te	0.262	*
	0.261	†
	0.264	§
As–As	0.262	*
	0.252	†
	0.257	[13]
	0.259	[21, 22]
	0.251	[23]
As–Te	0.257	*
	0.258	†
	0.258	[13]
	0.255	[21]
Te–Te	0.258	*
	0.262	†
	0.260	[24]
	0.257	[21]
	0.262	[15]

*MI.
†MII.
‡Estimation of the average value between the pure metal and Cu_2S [11].
§Estimation by means of Schomacker and Stevenson's formula [12].

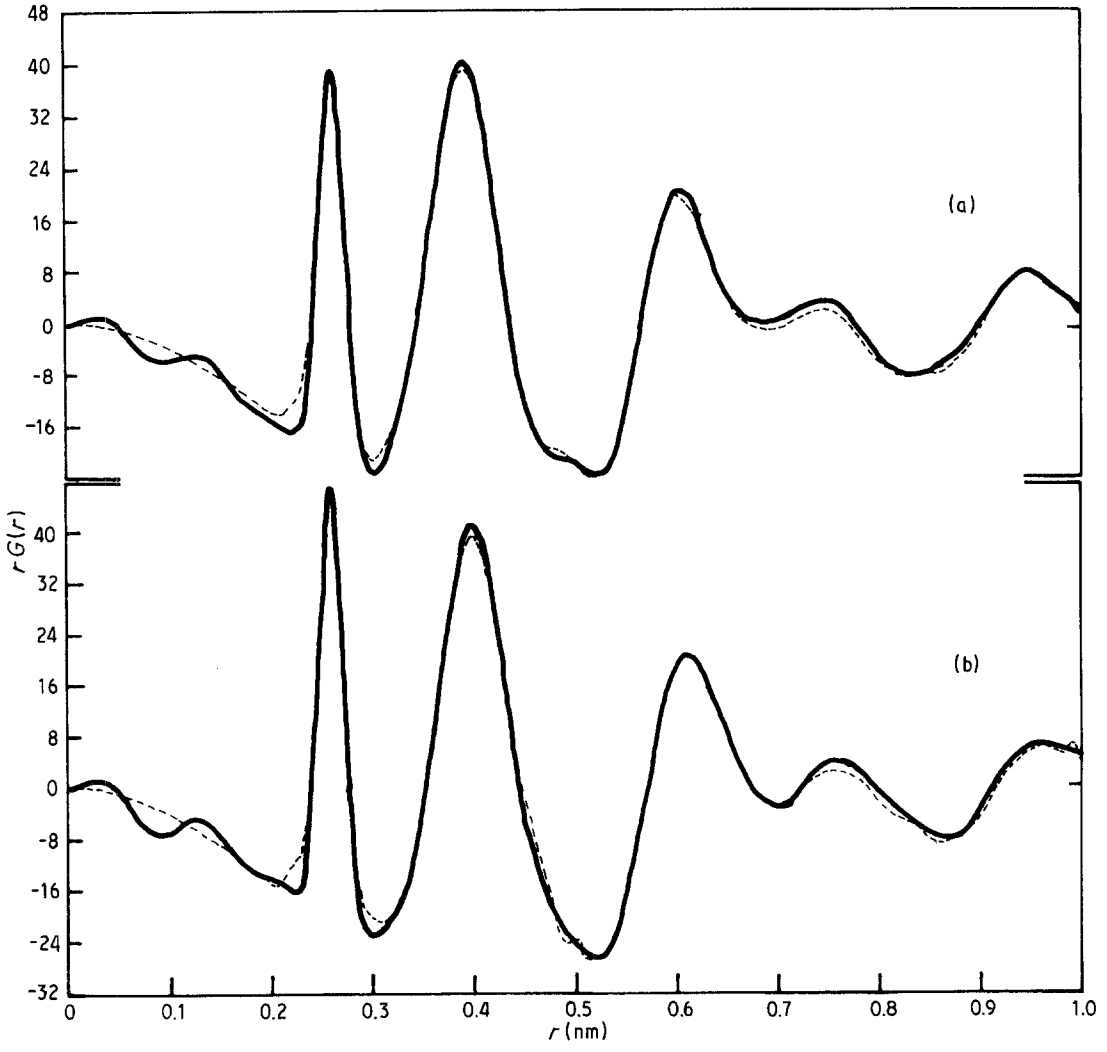

Figure 5 (——) Experimental and (– – –) model reduced RDFs for (a) MI and (b) MII, indicating the geometrical fitting of the models. For MI $\varepsilon^2 = 0.0171$ and for MII $\varepsilon^2 = 0.0215$.

differences found in electrical resistivity [20] must be attributed to Cu–X bonds with a greater ionization ability.

Table VI shows the average bonding distances (ABDs) that appear in both models together with some of the standard distances of similar alloys described in the literature. It is observed that the values obtained agree with data from the literature since, with the exception of the Cu–Cu ABD which are not considered statistically significant, all the other values differ less than 3% from those previously reported.

The similarity in ABDs between both models must be highlighted, as the mean value weighted with regard to bond numbers is an indication of the greater compactness of the model of Alloy MII, which is in agreement with the mean experimental coordination given by the RDF (2.44 ± 0.1 atoms for MI against 2.86 ± 0.1 for MII).

The ABDs of the Cu–Te and As–Te bonds are equal in both models, while the ABD of the Te–Te bond is greater in MII. This disagrees with the rest and may be related to lesser bonding of these atoms. Thus, Table VII shows the ABDs of tellurium atoms with coordination defects (Te(1) and Te(3)), bound to arsenic and tellurium atoms. However, for the Cu–Te bonds, insufficient ABDs have been established, and cannot be considered representative.

On one hand, ABD values higher than the average are observed for monocoordinated tellurium atoms of the MI model, indicating that the bonding energy is lower than the others. On the other hand, in the MII model, the ABD values agree with the average for the model. These results clearly indicate the weak bonding of tellurium atoms.

One should note the increase in the number of

TABLE VII Averaged bonding distances of tellurium atoms with coordination defects and number of these bonds (n) for every 100 atoms of material

Bond*	MI		MII	
	$\langle d \rangle$ (nm)	n	$\langle d \rangle$ (nm)	n
As–Te(1)	0.264	7	0.258	6
As–Te(3)	0.258	9	0.259	9
Te–Te(1)	0.262	4	0.262	1
Te–Te(3)	0.257	10	0.262	6

*Te(1) singly coordinated, Te(3) threefold coordinated.

TABLE VIII Averaged bonding angles (deg)

Type of angle	MI	MII
X–Cu–X	106.6	106.2
X–As–X	107.6	107.2
X–Te–X	110.3	108.1

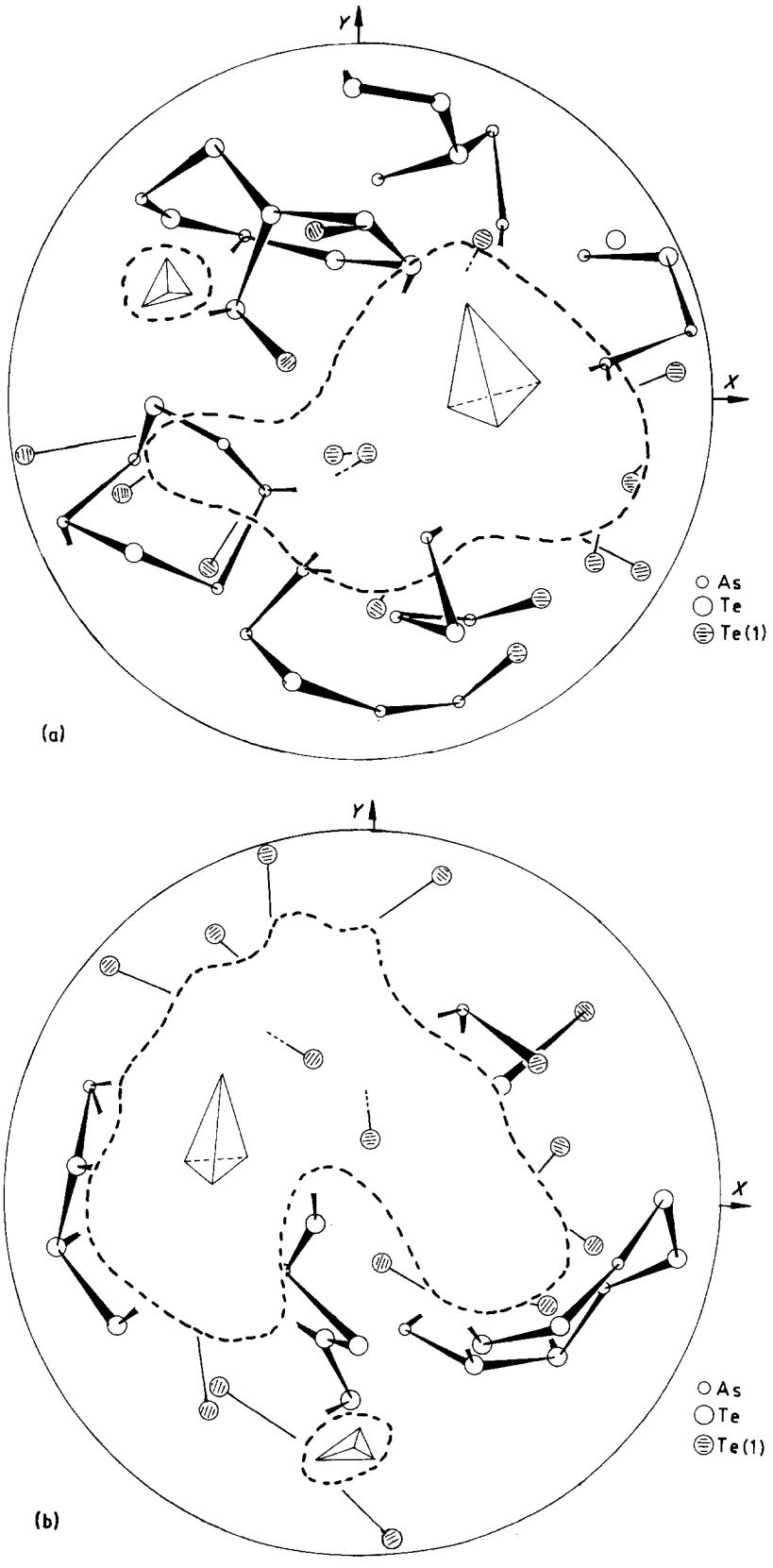

Figure 6 Schematic spatial representation of the tetrahedral clusters enclosed by the dotted line (centred on copper and some on arsenic atoms), together with atomic chains in the cluster voids and Te(1) atoms singly coordinated in the cluster periphery. (a) Model of MI alloy and (b) model of MII alloy.

Cu–X bonds in the Model MII in comparison to that of MI which is directly related to their electrical resistivity.

The bonding angle of each element with two first neighbours is also considered a parameter of structural interest. The mean values of the bonding angles for both models are set out in Table VIII.

In spite of the slight discrepancies with the characteristic angle (109.5°) of a regular tetrahedron, which in the least favourable case is no greater than 3%, all the indicated values may be considered acceptable for the models of the studied compositions, if it is taken into account that the first distortions that may be expected in the structure of an amorphous material are present in the bonding angles. It must also be pointed out that the angles with a vertex in the same element have very similar values in both models.

A spatial view of the tetrahedral network of the models of each alloy is shown in Figs 6a and b, where the similarity in both distributions may be appreciated as well as the greater compactness of the MII model.

5. Conclusions

The tridimensional structure of the present alloys may be described as a network of tetrahedra centred on copper, some also being centred on arsenic, thus making the atomic network more compact. In both cases the tetrahedral network is distributed in clusters, voids being mainly occupied by singly coordinated tellurium atoms. The distribution of inter-tetrahedral chains and rings affects the compactness of the atomic network.

References

1. Z. U. BORISOVA, "Glassy semiconductors" (Plenum, New York, 1981).
2. D. ADLER, B. B. SCHWARTZ and M. C. STEELE (Eds), "Physical properties of amorphous materials" (Plenum, New York, 1985).
3. J. VÁZQUEZ and F. SANZ, *Ann. Fis. B* **80** (1984) 31.
4. B. E. WARREN, "X-ray diffraction" (Addison-Wesley, Reading, 1969).
5. J. L. FINNEY, *Proc. R. Soc.* **A319** (1970) 479.
6. D. TURNBULL and D. E. POLK, *J. Non-Cryst. Solids* **8–10** (1972) 19.
7. M. METRÓPOLIS, A. W. ROSEBLUTH, M. N. ROSEBLUTH and A. M. TELLER, *J. Chem. Phys.* **21** (1953) 1087.
8. G. MASON, *Nature* **217** (1968) 733.
9. N. J. SHEVCHIK, PhD thesis, Harvard University (1972).
10. A. D'ANJOU and F. SANZ, *J. Non-Cryst. Solids* **28** (1978) 319.
11. R. B. HESLOP and K. JONES, "Inorganic Chemistry" (Elsevier, Amsterdam, 1976).
12. F. D. BLOSS, "Crystallography and Crystal Chemistry" (Holt, Rinehart and Winston, New York, 1977).
13. J. VÁZQUEZ, E. MÁRQUEZ, P. VILLARES and R. JIMÉNEZ-GARAY, *Mater. Lett.* **4** (1986) 360.
14. L. PAULING, "Uniones Quimicas" (Kapelusz, Buenos Aires, 1969).
15. L. ESQUIVIAS and F. SANZ, *J. Non-Cryst. Solids* **72** (1985) 165.
16. S. H. HUNTER, A. BIENNENSTACK and T. M. HAYES, "The Structure of Non-Crystalline Materials", edited by P. H. Gaskell (Taylor and Francis, London, 1977).
17. J. VÁZQUEZ, P. VILLARES and R. JIMÉNEZ-GARAY, *Mater. Lett.* **4** (1986) 485.
18. J. VÁZQUEZ, L. ESQUIVIAS, P. VILLARES and R. JIMÉNEZ-GARAY, *Ann. Fis. B* **81** (1985) 223.
19. M. A. KASTNER, D. ADLER and H. FRITZSCHE, *Phys. Rev. Lett.* **37** (1976) 1504.
20. M. M. HAIFZ, M. M. IBRAHIM and M. DONGOL, *J. Appl. Phys.* **54** (1983) 1950.
21. J. VÁZQUEZ, P. VILLARES and R. JIMÉNEZ-GARAY, *J. Non-Cryst. Solids* **86** (1986) 251.
22. A. J. APLING, A. J. LEADBETTER and A. C. WRIGHT, *ibid.* **23** (1977) 369.
23. S. ITOH, T. FUJIWARA and M. OKAZAKI, *ibid.* **50** (1982) 49.
24. J. VÁZQUEZ, P. VILLARES and R. JIMÉNEZ-GARAY, *Mater. Lett.* **4** (1986) 171.

Received 3 June
and accepted 27 July 1987